Long Stress (190 h) Operation of NO_2 p-Type Doped Diamond MOSFETs

Niloy Chandra Saha, Tomoki Shiratsuchi, Seong-Woo Kim, Koji Koyama, Toshiyuki Oishi, *Senior Member, IEEE*, and Makoto Kasu

***Abstract*— In this letter, we report the constant gate bias stress characteristics of an Al_2O_3 layer passivated, NO_2 p-type doped diamond metal-oxide-semiconductor field-effect transistor (MOSFET) for a long period of 190 h. The MOSFET exhibited stable operation throughout the period without any degradation in the drain current; rather the drain current gradually increased. Long stress time led to an increase in the gate leakage current, which can be attributed to the charge injection into the Al_2O_3 layer. Following the withdrawal of the stress, the gate leakage current disappeared as soon as the trapped charges in the Al_2O_3 layer were released and MOSFET characteristics recovered to their initial states. This study revealed the potential long-period stability and durability of diamond MOSFETs for power circuit applications.**

***Index Terms*—diamond MOSFET, p-type doping, stable operation, stress effects**

I. Introduction

DIAMOND is the ultimate ultra-wide bandgap semiconductor material for next-generation high-power and high-frequency transistors. Diamond has a high bandgap energy of 5.47 eV, including a high electric breakdown field >10 MV/cm, high thermal conductivity of 22 W/cm·K [1-3], and high carrier mobilities (electron and hole mobilities of 4500 and 3800 $cm^2V^{-1}s^{-1}$, respectively) [4]. The excellent radio frequency (RF) characteristics of diamond field-effect transistors (FETs) were reported with maximum RF power densities of 2.1 and 3.8 W/mm at 1 GHz [5, 6]. Moreover, high-frequency operation of diamond FETs demonstrated a maximum cut-off frequency (f_T) of 70 GHz [7] and a maximum frequency of oscillation (f_{max}) of 120 GHz [8].

The NO_2 p-type doping in hydrogen-terminated diamond (H-diamond) is demonstrated to generate hole carriers. The hole carrier concentration by NO_2 p-type doping is one order higher in magnitude (up to 2.4×10^{14} cm^{-2}) than that by air doping [9, 10]. Also, the Al_2O_3 passivation layer over the hole channel prevents the desorption of NO_2 molecules and thermal degradation [11]. An Al_2O_3 layer passivated, NO_2 p-type doped H-diamond metal–oxide– semiconductor field-effect-transistor (MOSFET) exhibited the highest drain current density of 1.35 A/mm [12]. The highest breakdown voltage of diamond MOSFETs was reported as 3659 V [13]. Furthermore, diamond MOSFETs were demonstrated for high-power operation with a maximum Baliga's figure-of-merit of 875 MW/cm^2 [14].

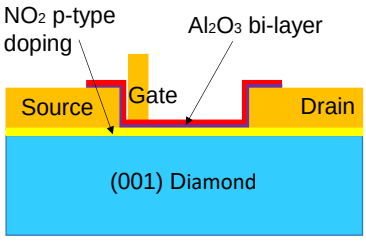

Fig. 1. Schematic cross-section of the Al_2O_3 passivated NO_2 p-type doped diamond MOSFETs.

The stable operation of diamond transistors is the essential realization for power circuit applications. The reliability and durability characterization of diamond MOSFETs over a long period is yet to be reported. Furthermore, on-state reliability testing is necessary to comprehend the potential mechanism of drain current degradation and the failure of MOSFETs over time. For the first time, this study reports stable long-stress characteristics of a NO_2 p-type doped diamond MOSFET for a long period of 190 h. Moreover, the changes in the output characteristics due to stress and its recovery to the initial state are discussed.

II. Growth and Device Fabrication

Fig. 1 shows the cross-section of a diamond MOSFET with NO_2 p-type doping and Al_2O_3 layer fabricated on (001) diamond substrates misoriented by 3.0° toward the [110] direction. The freestanding misoriented diamond layer was grown heteroepitaxially on an Ir buffered misoriented (11$\bar{2}$0) A-plane sapphire substrates [15]. An approximately 100-nm thick diamond layer was grown on the diamond substrates via microwave plasma chemical vapor deposition. The microwave plasma power was 750 W. The ratio of CH_4/H_2 was 1% and the working pressure was 50 Torr. The H-diamond sample surface was exposed to 2% NO_2 gas (diluted in N_2) to carry out the NO_2 p-type doping. For ohmic contact formation, a 50-nm-thick Au layer was deposited. The photolithographically patterned active channel was again exposed to NO_2 gas to retain the high hole concentration that was reduced during the fabrication processes [14].

A 16-nm thick Al_2O_3 bilayer was deposited via atomic layer deposition technique to passivate the active channel. The initial 4-nm-thick Al_2O_3 layer was deposited at 120 °C to ensure minimum desorption of NO_2 during the sample heating,

Manuscript received February 03, 2023. This work was supported by the Japan Society for the Promotion of Science Grants-in-aid for Scientific Research (No. 22H01974).

N. C. Saha, T. Shiratuschi, T. Oishi, and M. Kasu are with the Department of Electrical and Electronic Engineering, Saga University, Saga 840-8502, Japan (e-mail: kasu@cc.saga-u.ac.jp).

S. -W. Kim, and K. Koyama are with Orbray Co., Ltd. Tokyo 123-8511, Japan.

followed by the second 12-nm-thick Al_2O_3 layer at 230 °C to improve the overall quality of the Al_2O_3 layer. The Al_2O_3 bilayer also serves as the gate-insulating layer. For the gate formation, a 50-nm-thick Au layer was evaporated, and the gate was placed adjacent to the source contact [16]. The MOSFET has a gate length (L_G) of 2 µm, gate width (W_G) of 45 µm, source to drain length (L_{SD}) of 14.5 µm, and the gate to drain length (L_{GD}) was 12.5 µm. The source, gate, and drain electrodes of the diamond sample were bonded to a printed circuit board for lifetime measurement.

The output characteristics and stress characteristics measurements of the MOSFET were performed using the Keysight 1505A power device analyzer. The measurement was performed in air at room temperature (RT).

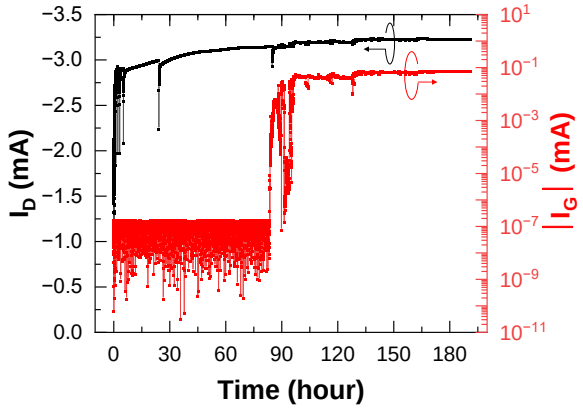

Fig. 2. Stress time dependence of the drain and gate current of the NO_2 p-type doped diamond MOSFET under gate bias of −2 V and drain of −10 V.

III. Results and Discussion

Fig. 2 shows the time dependence of the stress measurements. A gate bias (V_{GS}) of −2 V and drain bias (V_{DS}) of −10 V were applied to the MOSFET, and the drain current (I_D) and gate current (I_G) were measured as a function of the stress time. Stress measurements obtained over a long period (190 h) showed no degradation in the drain current; rather a gradual increase was observed. At the beginning of the stress measurement, I_D was 2.1 mA and I_G was approximately $\leq 1.6 \times 10^{-7}$ mA. Although I_D gradually increased during the stress, I_G was almost constant. However, after 83 h of stress, I_G abruptly increased by almost five orders in magnitude. This increase in I_G did not affect I_D.

The dc output and transfer characteristics were measured during short-time (<30 s) interruptions of one stress measurement. Therefore, the spikes (sudden changes) in drain current appeared in Fig. 2 were due to a slight change in characteristics (the recovery phenomenon described later) during the stress-measurement interruptions. The output characteristics were measured at different stress period intervals. During the initial five hours of stress measurements, the output characteristics were measured at a combination of 1, 5, 10-, 30-, 60-, and 120-min intervals. Subsequent two measurements were performed after 24 h and 190 h of stress. Even after a total of 190 h stress operation, the device remained unbroken, which enabled us to investigate the recovery stage of the MOSFET characteristics.

Figs. 3 (a), (b), (c), and (d) show the DC output characteristics of the diamond MOSFET before stress, after 190 h of stress, after 30 min of recovery, and after 5 h of recovery, respectively. Before applying the stress, the maximum I_D was measured as 54.4 mA/mm with an on-resistance R_{ON} of 160 Ω·mm. Although 190 h of stress resulted in higher I_D, a higher gate leak also appeared. This I_D was measured immediately without any delay after 190 h of stress. In addition, a negligible change in device temperature (<1 °C) due to stress was confirmed using a Nippon Avionics infrared camera R500EX, probably because the dissipation power of the diamond MOSFET was very low. Furthermore, diamond has a very high thermal conductivity. Within 30 min of the recovery period, gate leakage disappeared, and I_D and R_{ON} recovered to their initial values. However, following 5 h of recovery, the same output characteristics demonstrate the excellent resilience of the MOSFET.

The transfer characteristics and gate leakage currents (see Figs. 4(a) and (b), respectively) during stress and after stress were measured at V_{DS} =−10 V, as shown in Fig. 4. The on/off ratio of the MOSFET before applying any stress was $>10^6$ with a considerably low I_G. After 24 h of stress, the on/off ratio and I_G remained the same; however, I_D was found to be increased. At the end of 190 h of stress operation, the on/off ratio was significantly reduced to ~48 because of the high I_G. The withdrawal of stress showed that the on/off ratio was increasing and after 30 min, I_D and I_G recovered to their initial states. These phenomena indicate that a temporary leak path was

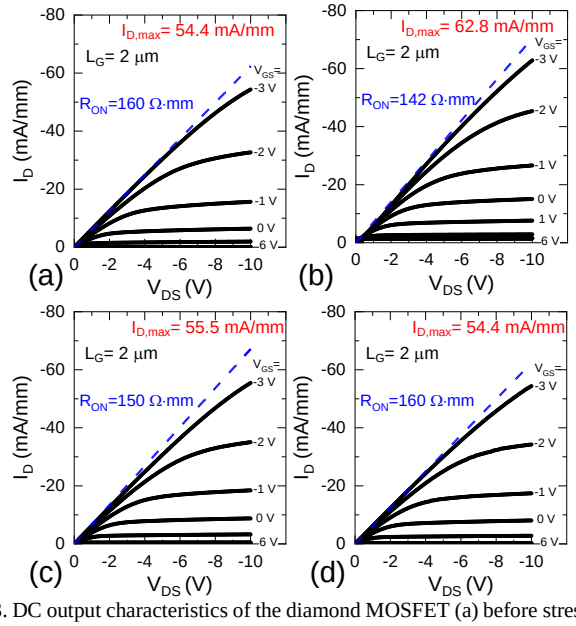

Fig. 3. DC output characteristics of the diamond MOSFET (a) before stress, (b) after 190 h of stress, after recovery time of (c) 30 min, and (d) 5 h.

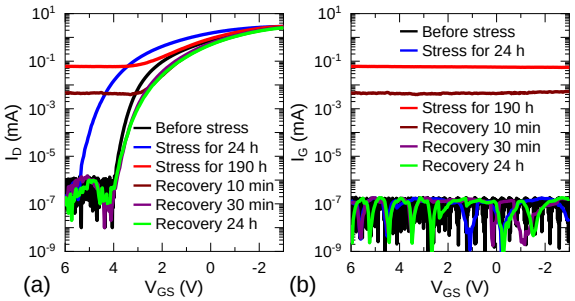

Fig. 4. (a) Transfer characteristics (I_D-V_{GS}) and (b) gate currents (I_G-V_{GS}) of the diamond MOSFET at different stage of stress and recovery period.

formed across the Al_2O_3 layer due to the stress which recovered as the stress was withdrawn.

From the transfer characteristics, the threshold voltage (V_{th}) values were determined by linearly extrapolating the $\sqrt{I_D}$–V_{GS} characteristics. Fig. 5(a) shows the changes in threshold voltages (ΔV_{th}) during the stress and recovery times. Here, ΔV_{th} is defined as the $\Delta V_{th} = V_{th,measured} - V_{th,initial}$. The $V_{th,initial}$ is the V_{th} that was measured before applying the stress. The $V_{th,measured}$ values are the V_{th} measured during stress and recovery time. As the stress time was increasing, ΔV_{th} was shifting toward more positive values, indicating that the V_{th} was increasing. The increase in V_{th} can be explained as the increase of hole carriers which requires a higher voltage to deplete. The gradual increase of drain current during the stress could be a probable reason for this shift in ΔV_{th}.

During the recovery period, ΔV_{th} sharply declined to the negative level following the removal of stress, which can be attributed to the high gate leakage that increased due to stress. After 30 min of recovery period (when the gate leakage current recovered to its initial values), ΔV_{th} started to increase; however, it did not reach the initial value (0 V). A long period of stress could lead to a change of charges in the Al_2O_3 layer, which might cause the shift of V_{th} toward the negative gate bias.

Fig. 5 (b) shows the interfacial state density (D_{it}) during the stress and recovery time. The subthreshold swing was determined from the transfer characteristics and then translated into D_{it}. There are no major changes observed in D_{it} up to 24 h of stress time. However, it increased by one order of magnitude between 24 h and 190 h of the stress period and decreased to the initial value within 30 min of stress removal. Furthermore, no substantial changes in D_{it} were observed within the subsequent 48 h of recovery.

During the stress period, charges enter into the Al_2O_3 layer that could act as the negative fixed charges and are responsible for increasing hole carriers, which increases I_D and V_{th}. The quantity of charges could be a function of the stress time. The excessive injection of charges into the Al_2O_3 layer owing to the longer stress time (~ 83 h of stress) may result in a temporary leak path across the Al_2O_3 layer. However, unstable fluctuations of the injected charges from 83−96 h of stress are realized by monitoring the fluctuation of I_G (in Fig. 2) during that period of stress. An increased gate-leak current flows from the gate to the diamond through this leak path. Furthermore, constant charge flow (gate leakage current flow) through the Al_2O_3 layer causes additional temporary defects at the Al_2O_3/diamond interface; therefore, a rise in D_{it} was observed after 190 h of stress.

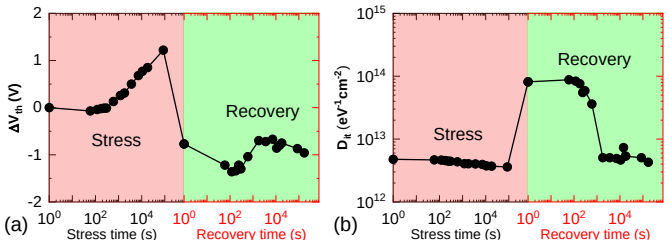

Fig. 5. Stress and recovery time dependance of (a) ΔV_{th} and (b) D_{it}. of the diamond MOSFET

Following the withdrawal of the stress, trapped charges in the Al_2O_3 layer and hole carriers at the Al_2O_3/diamond interface were started to release. Depending on the trap emission time and trap location, recovery time may vary [17]. In our study, it takes approximately 30 min to disappear I_G and recover I_D and D_{it} to their initial values. The recovery time is likely to be attributed to the emission time of the trapped charges in the Al_2O_3 layer. In addition, we speculate that the determined D_{it} values are associated with the border trap density [18]. Border traps are charges trapped in the Al_2O_3 layer near the interface that have a longer emission time constant than that of interface traps. This could be a possible reason for long recovery times of D_{it}.

IV. Conclusions

This study manifested the long-time stress measurement of a NO_2 p-type diamond MOSFETs for the first time. The changes during the stress and effects of stress were studied in terms of the drain current, gate current, threshold voltages, and interfacial states. 190 h of stress operation showed, there was no degradation in I_D, though an increase in I_G was observed after 83 h of stress because of charge injection into the Al_2O_3 layer. Following 190 h of stress operation, a substantial increase in interfacial states was obtained with a low on/off ratio caused by the increased I_G during the stress. However, the MOSFET characteristics were recovered after 30 min of stress removal, which suggests the durability of diamond MOSFETs for long-period operation in power circuit applications.

References

[1] M. W. Geis, "Growth of device-quality homoepitaxial diamond thin films," *MRS Proc*, vol. 162, pp. 15–22, 1989, DOI: 10.1557/PROC-162-15.

[2] C. J. Wort and R. S. Balmer, "Diamond as an electronic material," *Mater. Today*, vol. 11, no. 1–2, pp. 22–28, Jan. 2008, DOI: 10.1016/S1369-7021(07)70349-8.

[3] Y. Yamamoto, T. Imai, K. Tanabe, T. Tsuno, Y. Kumazawa, and N. Fujimori, "The measurement of thermal properties of diamond," *Diam. Relat. Mater.*, vol. 6, no. 8, pp. 1057–1061, May 1997, DOI: 10.1016/S0925-9635(96)00772-8.

[4] J. Isberg, J. Hammersberg, E. Johansson, T. Wikström, D. J. Twitchen, A. J. Whitehead, S. E. Coe, and G. A. Scarsbrook, "High carrier mobility in single-crystal plasma-deposited diamond," *Science*, vol. 297, no. 5587, pp. 1670–1672, Sep. 2002, DOI: 10.1126/science.1074374.

[5] M. Kasu, K. Ueda, H. Ye, Y. Yamauchi, S. Sasaki, and T. Makimoto, "2 W/mm output power density at 1 GHz for diamond FETs," *Electron. Lett.* vol. 41, no. 22, p. 1249, Oct. 2005, DOI: 10.1049/el:20053194.

[6] S. Imanishi, K. Horikawa, N. Oi, S. Okubo, T. Kageura, A. Hiraiwa, and H. Kawarada, "3.8 W/mm RF power density for ALD Al_2O_3-based two-dimensional hole gas diamond MOSFET operating at saturation velocity," *IEEE Electron Device Lett.*, vol. 40, no. 2, pp. 279–282, Dec. 2019, DOI: 10.1109/led.2018.2886596.

[7] X. Yu, J. Zhou, C. Qi, Z. Cao, Y. Kong, and T. Chen, "A high frequency hydrogen-terminated diamond MISFET with f_T/f_{MAX} of 70/80 GHz," *IEEE Electron Dev. Lett.*, vol. 39, no. 9, pp. 1373–1376, Aug. 2018, DOI: 10.1109/LED.2018.2862158.

[8] K. Ueda, M. Kasu, Y. Yamauchi, T. Makimoto, M. Schwitters, D. Twitchen, G. Scarsbrook, and S. Coe, "Diamond FET using high-quality polycrystalline diamond with f_T of 45 GHz and f_{max} of 120 GHz," *IEEE Electron Dev. Lett.*, vol. 27, no. 7, pp. 570–572, Aug. 2006, DOI: 10.1109/LED.2006.876325.

[9] M. Kubovic, M. Kasu, H. Kageshima, and F. Maeda, "Electronic and surface properties of H-terminated diamond surface affected by NO_2 gas," *Diam. Relat. Mater.*, no. 7, pp. 889–893, Sep. 2010, DOI: doi.org/10.1016/j.diamond.2010.02.021.

[10] T. Wade, M. W. Geis, T. H. Fedynyshyn, S. A. Vitale, J. O. Varghese, D. M. Lennon, T. Grotjohn, R. J. Nemanich, and M. A. Hollis, "Effect of surface roughness and H–termination chemistry on diamond's

semiconducting surface conductance," *Diam. Rel. Mater.*, vol. 76, pp. 79–85, Jun. 2017, DOI: 10.1016/j.diamond.2017.04.012.

[11] M. Kasu, H. Sato, and K. Hirama, "Thermal stabilization of hole channel on H-terminated diamond surface by using atomic-layer-deposited Al_2O_3 overlayer and its electric properties," *Appl. Phys. Express*, vol. 5, no. 2, p. 025701, Feb. 2012, DOI: 10.1143/apex.5.025701.

[12] K. Hirama, H. Sato, Y. Harada, H. Yamamoto, and M. Kasu, "Diamond field-effect transistors with 1.3 A/mm drain current density by Al_2O_3 passivation layer," *Jpn. J. Appl. Phys.*, vol. 51, no. 9R, pp. 090112, Aug. 2012, DOI: 10.7567/jjap.51.090112.

[13] N. C. Saha, S.-W. Kim, K. Koyama, T. Oishi, and M. Kasu, "3659-V no2 P-type doped diamond MOSFETs on misoriented heteroepitaxial diamond substrates," *IEEE Electron Device Letters*, pp. 1–1, Dec. 2022, DOI: 10.1109/LED.2022.3226426.

[14] N. C. Saha, S.-W. Kim, T. Oishi, and M. Kasu, "875-MW/cm² Low-Resistance NO_2 p-Type Doped Chemical Mechanical Planarized Diamond MOSFETs," *IEEE Electron Dev. Lett.*, vol. 43, no. 5, pp. 777–780, May 2022, DOI: 10.1109/LED.2022.3164603.

[15] S.-W. Kim, R. Takaya, S. Hirano, and M. Kasu, "Two-inch high-quality (001) diamond heteroepitaxial growth on sapphire ($11\bar{2}0$) misoriented substrate by step-flow mode," *Appl. Phys. Express*, vol. 14, no. 11, p. 115501, Oct. 2021, DOI: 10.35848/1882-0786/ac28e7.

[16] N. C. Saha and M. Kasu, "Improvement of the Al_2O_3/NO_2/H-diamond MOSFET by using Au gate metal and its analysis," *Diam. Relat. Mater.*, vol. 92, pp. 81–85, Feb. 2019, DOI: 10.1016/j.diamond.2018.12.017.

[17] Z. Chen, X. Yu, J. Zhou, S. Mao, Y. Fu, B. Yan, R. Xu, Y. Kong, T. Chen, Y. Li, and Y. Xu, "Negative constant voltage stress-induced threshold voltage instability in hydrogen-terminated diamond MOSFETs with low-temperature deposited Al_2O_3," *Applied Physics Letters*, vol. 117, no. 13, p. 133501, Sep. 2020, DOI: https://doi.org/10.1063/5.0020136.

[18] N. C. Saha and M. Kasu, "Heterointerface properties of diamond MOS structures studied using capacitance–voltage and conductance–frequency measurements," *Diamond and Related Materials*, vol. 91, pp. 219–224, Jan. 2019, DOI: doi.org/10.1016/j.diamond.2018.11.019.